La mer 34: 152–162, 1996
Société franco-japonaise d'océanographie, Tokyo

Separation of the Tsushima Current from the Kuroshio: A numerical study with an idealized geometry

Soo Yong NAM*, Moon-Sik SUK*, Inkweon BANG*, Kyung-Il CANG* and Young-Ho SEUNG**

Abstract: The dynamics on the separation of the Tsushima Current from the Kuroshio is studied using a three dimensional primitive equation model with an idealized domain which consists of a continental shelf and a marginal sea in the north and a deep ocean in the south with a stepwise topographic change between them. The model ocean is vertically stratified initially and a sinusoidal wind stress is applied only over the deep ocean to establish an anticyclonic circulation. For a weakly inertial case with a zonally oriented shelf break, a part of the western boundary current is separated in the eastern part of the continental shelf, the western rim of an island which the marginal sea ane enters the marginal sea, which differs from a barotropic model result predicting the separation along the western wall of the continental shelf. Numerical experiments show that the branching position is controlled by the orientation of the shelf break and the nonlinearity of the western boundary current. On the other hand, the volome transport of the inflow into a marginal sea is little affected by the nonlinearity of the WBC, the orientation of the shelf break and the specific topographic features of the shelf break, but by the transport of the western boundary current and the depth ratio beween the marginal sea and the deep ocean as other studies suggested.

1. Introduction

The Kuroshio flows northeastward along the continental shope of the East China Sea (ECS henceforth) and part of it overruns the shelf break to form the Tsushima Current (TC henceforth) which enters the East Sea (or Sea of Japan, ES henceforth) through the Korea Strait. Its volome transport through the Korea Strait is estimated to be less than 4.0 Sy (MORIYASU, 1972; YI, 1966; MIITA and OGAWA, 1984) That is only 10% of the Kuroshio Transport in the ESC (ICHIKAWA and BEARDSLEY, 1993).

There seems to be two different views about the origin of the TC; one suggests that the TC originates from the northeastern area of Taiwan and/or the Taiwan Strait (BEARDSLEY *et al.*, 1985; GUAN, 1986; HSUEH, 1986; CHAO, 1991) and the others show that it comes from the west of Kyushu Island (GUO *et al.*, 1990; LIE and CHO, 1994; LIE *et al.*, 1993; LIM, 1971) by analyzing the hydrographic and satellite-tracked drifter data observed in the local area west of Kyushu Island. Barotoropic model results show that all of the TC water comes from the northeast of Taiwan and/or the Taiwan Strait as the Kuroshio impinges on the sloping topography (CHANG, 1993; SEUNG and NAM, 1992), which seems to suport the former view. A similar penetration of the Kuroshio takes place in a primitive equation model of the North Pacific (TAKANO and MISUMI, 1990), which has $1° \times 1°$ resolution in the horizontal and 6 levels in the vertical.

The penetrative flux into a marginal sea (MS henceforth) from the western boundary current (WBC henceforth) has been shown to be dependent on various factors. MINATO and K IMURA (1980) first quantified the flux in an idealized domain analytically using a linear frictional model. SEUNG and NAM (1992) examined the factors affecting the volume transport of the TC using a barotropic numerical model. The influx to a MS is dependent on the

* KORDI, Ansan P. O. Box 29, Seoul 425-600, Korea
** Dept. of Oceanography, INHA University, Incheon 402-751, Korea

transport of the WBC, depth ratio between a MS and a deep ocean and frictional parameterization but little affected by local winds over the continental shelf according to the above studies. CHANG (1993) pointed out that the changes in the wind stress over the deep ocean also influence the amount of influx using a barotropic model. NOF (1992) further showed analytically that the flux is a function of the latitude of the inflowing gap, the separation latitude of the Kuroshio and the stratification in the Pacific using a inviscid, inertial reduced-gravity model. No attempt has been made to investigate factors affecting the influx under a continuously stratified condition. The topographic and baroclinic influences play an important role in increasing the transport of the WBC (HOLLAND, 1973), hence likely affect the generation and the volume transport of the TC.

Although a primitive equation model (TAKANO and MISUMI, 1990) includes the ECS and the ES in its model domain the model resolution is not enough to examine the circulation in the above areas in detail. This study aims to examine the factors affecting the branching area of the WBC and the influx to a MS under a continuously stratified condition using a three dimensional numerical model. The model domain is simplified and thus made feasible to parameter studies. Model description and details of numerical experiments are described in Chapetr 2. Results of the each experiment are discussed in Chapters 3 and 4 focusing on the branching of the WBC and factors affecting the transport into a MS in Chapter 4 respectively. Chapter 5 provides a summary and discussions.

2. Model description

The numerical model used for the study is a primitive equation model by COX (1984). The governing equations are given by the continuity and conservation of momentum and density. The rigid-lid, hydrostatic and Boussinesq approximations are used for the foumulation of the equations. Under the Boussinesq approximation, variations in density are ignored where ρ appears as a coefficient but is takeninto account in the gravitational buoyancy force. High speed external gravity waves are filtered out due to the rigid-lid approximation. The model uses the B-grid configuration and the finite differencing is such that mass, heat, salt, variances of temperature, salinity and total energy are conserved in the model domain. Under the rigid-lid approximation, the external mode of momentum may be represented by a volume stream function ϕ. A prognostic equation for ϕ can be obtained by the vertical average of the momentum equations. This vorticity tendency equation is solved by successive-over-relaxation mothod and stream function over islands are obtained using the Hole Relaxation Method (TAKANO, 1974). Other detailed descriptions about the model are referred to COX (1984). where τ^x is the zonal wind stress, τ^y the meridional wind stress, τ_0 the maximum wind stress, L the meridional distance of the model domain, and l_1 the distance between the southern boundary and the separation latitude of the WBC.

The model ocean consists of a deep ocean in the south and a continental shelf and a MS in the north as shown in Fig. 1. The model domain covers 15°N–42°N, 120°E–150°E. The MS is connected with the deep ocean to the north and with the shelf to the south through two 100 km (north) and 200km (south) wide straits resepctively. The bottom of both the continen-

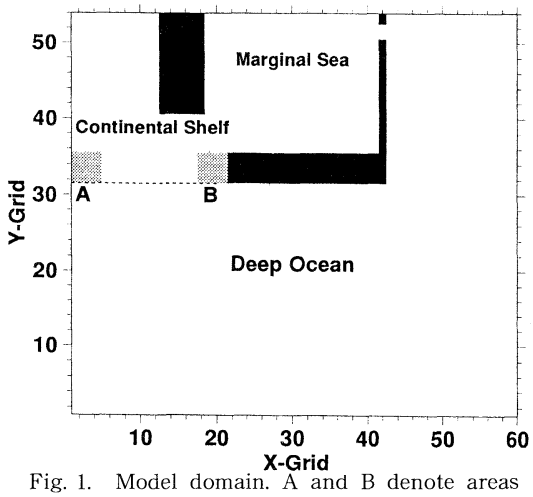

Fig. 1. Model domain. A and B denote areas where the branching of the WBC occurs depending on some parameters. The dashed line shows the location of step-like shelf break.

tal shelf and deep ocean is flat and the depths of both regions are 100m and 500m respectively. The depth of the MS is set to be the same as the depth of the continental shelf and there is no topographic irregularity within the MS, since a detailed circulation feature within the MS is beyond the scope of this study. However, the depth of the deep ocean is taken variable to examine the effect of depth difference between the two regions. The depth change between the deep ocean and the continental shelf takes place over one grid spacing so that it has a step-like character. The shelf break is placed in the east-west direction unless otherwise stated. Shaded parts in Fig. 1 on the continental shelf denote the areas where the branching of the WBC occurs depending on some parameters and will be referred to as an area A and area B respectively. Horizontally, the model domain is divided into $0.5^\circ \times 0.5^\circ$ grids, and there are 13 levels in the vertical as shown in Table 1. Salinity is held constant throughout the integration in all experiments and water density is calculated using a Knudsen's formula. The initial temperature profile increases linearly from 8℃ at the bottom to 20℃ at the surface of the deep ocean as shown in Table 1. Higher surface temperature (26℃) is imposed along the southern boundary of the model during time integration in order to maintain the vertical stratification. Without the supply of high temperature surface water, the stratification weakens and the model ocean is gradually cooled during time integration due to the advection and diffusion of upwelled cold water along the boundaries.

The values of lateral viscosity (Am) and diffusivity (Ah) are taken as 1×10^8 cm^2/sec and 5×10^7 cm^2/sec respectively, unless stated otherwise, and we use constant values of vertical viscosity and diffusivity of 1 cm^2/sec. The model domain is closed and no slip condition is imposed along all solid boundaries. The normal gradients of T and S are set to zero on the side of walls, at the surface and at the ocean bottom so that there are no heat and salt fluxes across these boundaries. The bottom stress is parameterized by the quadratic drag law with a drag coefficient of 0.0015. A simple type of wind-stress is applied only over the deep ocean

Table 1. Level thicknesses and initial temperatures and salinities

No. of Level	Thickness (m)	Temperature (℃)	Salinity (psu)
1	10	20.0	34.5
2	10	19.7	34.5
3	10	19.0	34.5
4	20	18.3	34.5
5	25	17.5	34.5
6	25	16.7	34.5
7	25	16.0	34.5
8	25	15.0	34.5
9	50	14.0	34.5
10	50	13.0	34.5
11	50	12.0	34.5
12	100	10.0	34.5
13	100	8.0	34.5

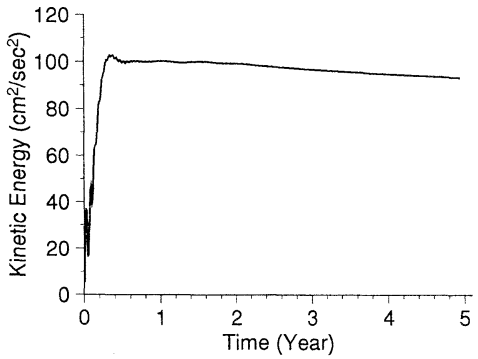

Fig. 2. Time series of total kinetic energy

to establish an asymmetric double gyres (e.g. subtropical and subpolar gyre), i.e.,

$$\tau^x = \tau_0 \cos\left(\frac{\pi(y-l_1)}{l_1}\right), \tau^y = 0, where\ 0 \le y \le L$$

Elven numerical experiments are conducted to study the variation of the branching area of the WBC and the transport of an inflow into the MS as listed in Table 2. Additionally, barotropic versions of EXP 8 are carried out to identify the role of stratification. For these barotropic versions the wind stress is applied in a depth-independent manner like a body force so the flow is two-dimensional. Fig. 2 shows an example of a time series of total kinetic energy averaged over the whole volume. The kinetic energy changes little after one year though it slightly decreases afterwards. In all experiments, numerical integrations are carried out for five years and the results of year five are presented since we are only interested

Table 2. Description of numerical experiments

	τ_0 (dyne/cm^2)	D (m)	A_m (cm^2/sec)	AA (°)	
EXP 1	2	500	1×10^8		
EXP 2	1				
EXP 3	4				
EXP 4					deep trough in area A
EXP 5					deep trough in area A
EXP 6			5×10^7		
EXP 7			1×10^7		
EXP 8				30	
EXP 9		250			
EXP 10		700			
EXP 11		1000			

* D denotes the depth of the deep ocean and AA the angle of the shelf break measured in the anticlockwise direction from the east.

in the steady solution.

EXP 1 is a nonlinear standard experiment, in which the shelf break is oriented in a purely zonal direction. The maximum wind stress applied over the deep ocean is halved (EXP 2) or doubled (EXP 3) in order to decrease or increase the volume transport of the WBC, respectively, and to examine the resultant changes in the branching position of the WBC and the transport of the inflow into the MS. A rectangular deep trough is introduced in area B (EXP 4) in Fig. 1 as like the deep trough west of Kyushu and in area A (EXP 5) to see whether it affects the branching of the WBC. OEY and CHEN (1991) suggests that the deep trough west of Kyushu Island contibutes to the variability of the TC. In EXP 6 and EXP 7, the nonlinearity of the WBC is made to increase by decreasing the horizontal eddy viscosity coefficient. The orientation of the continental shelf break northeast of Taiwan is not zonal but tilted in the northeast direction, hence the Kuroshio is incident on a sloping shelf break northeast of Taiwan. The influence of the sloping topography on the penetration of the WBC is examined in EXP 8. Effects of the depth ratio between the deep ocean and the shelf are investigated in EXP 9 to EXP 11.

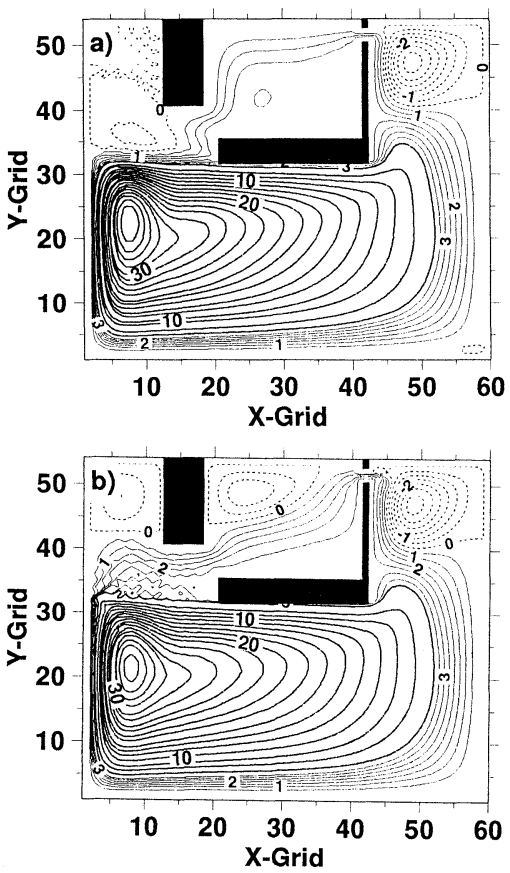

Fig. 3. Contours of streamfunction in Sv($\times10^6$ m^3/s) unit for a) EXP 1 and b) the barotropic version with all parameters the same as in EXP 1. The contour intervals are 0.5 Sv between −4 Sv to 4 Sv and 2 Sv elsewhere. The dashed lines denote the negative values of streamfunction.

3. Separation of the Tsushima Current

Figure 3 shows streamlines of EXP 1 and its baropropic version. An anticyclonic gyre is established south of the grid point 40 in the deep ocean and a much weaker cyclonic subpolar gyre north of it. The separation latitude of the

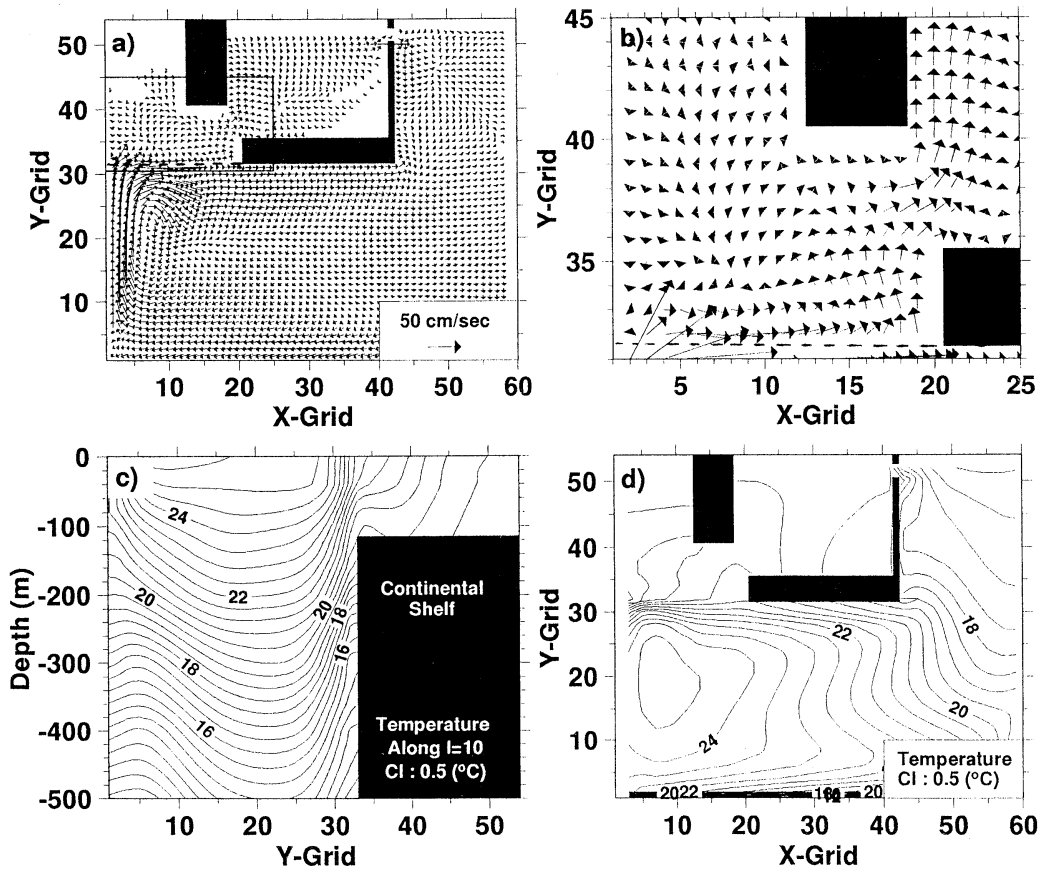

Fig. 4. Plots of a) currents at 75 m in whole basin, b) enlarged currents at 75 m in the continental shelf region, c) the vertical profile of temperature along i=10 in Fig. 1 and d) the horizontal distribution of temperature for EXP 1. The dashed line denotes the shelf break.

WBC coincides with the zero wind curl latitude. The WBC the subtropical gyre due to the planetary β-effect is formed in the deep ocean, the maximum volume transport of which is about 40 Sv in EXP 1 and is about 36 Sv in the barotropic version respectively. The stratification acts to increase the transport of the WBC. The WBC in the standard experiment is weakly inertial with the Reynolds number, $R_e = VW/A_m \approx 9$, whele $V \approx 60$cm/sec is the maximum northward velocity along the western wall of the deep ocean (Fig. 4a), and $W \approx 150$ km, half-width of the WBC. Most of the WBC flows eastward along a zonally-oriented shelf break in both EXP 1 and the barotropic version.

Remarkable changes in the penetration of the WBC and the circulation on the shelf can be seen in both experiments. For a stratified case of EXP 1, part of the WBC is separated in area B (Fig. 3a) and enters the MS, and a weak and isolated cyclonic circulation cell is induced on the continental shelf just north of the shelf break. On the other hand for the barotropic version, the separation takes place in area A and most of the WBC which penetrates onto the shelf enters the MS after turning anticyclonically in the shelf, while part of it rejoins the WBC. The cyclonic circulation cell on the shelf is located farther to the north in the barotropic experiment than in the baroclinic one. The cyclonic circulation on the shelf seems to result from the diffusion of the positive vorticity along the inshore part of the WBC. The volume transport into the MS is 1.86 Sv in EXP 1 and 2.8 Sv in the barotropic version, hence the stratification reduces the

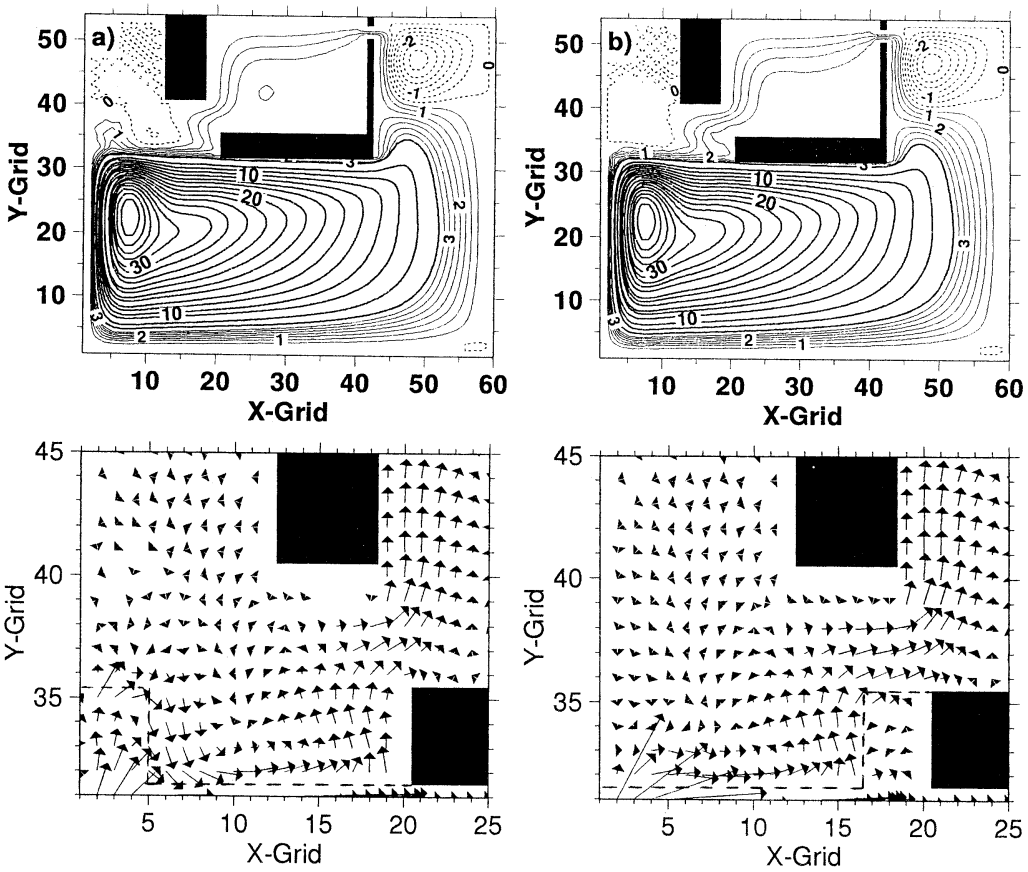

Fig. 5. Contours of streamfunction in Sv ($\times 10^6 m^3/s$) unit for a) EXP 4 and b) EXP 5. Here the retangular-shaped deep trough is introduced in area A (EXP 4) and are B (EXP 5). Lower panels are enlarged currents in the continental shelf region. The dashed line denotes the shelf break.

transport into the MS while it acts to increase the transport of the WBC.

The horizontal temperature distribution in Fig. 4d shows much the same large scale features as the streamfunction plot. High temperature core is located just offshore of the WBC where the local recirculation gyre appears, and temperature is low in the subpolar region and along the southern boundary due to the upwelling of the cold water from the lower layer. A thermal front is formed along the shelf break and the intrusion of warm water to the MS can be seen in area B. Vertical profile of temperature along a meridional section also shows the shelf break frontal structure (Fig. 4c). The shelf water becomes vertically homogeneous despite the initial stratification. The computed vertical profile of temperature is similar to published observations in the ECS in winter.

A rectangular-shaped deep trough is introduced in area A (EXP 4) and area B (EXP 5). Although the deep trough acts to guide part of the WBC onto the shelf in area A in EXP 4, the inflow into the MS originates from the area B as in the standard experiment (Fig. 5b). When the trough is located in area B like the trough west of Kyushu Island, the separation mainly takes place along the left flank of the trough and the flow inside the trough is weak and directed to the north (Fig. 5a). Recent ARGOS drifter trajectories clearly showed that the TC branches off the western flank of the deep trough west of Kyushu Island (Lie and Cho,

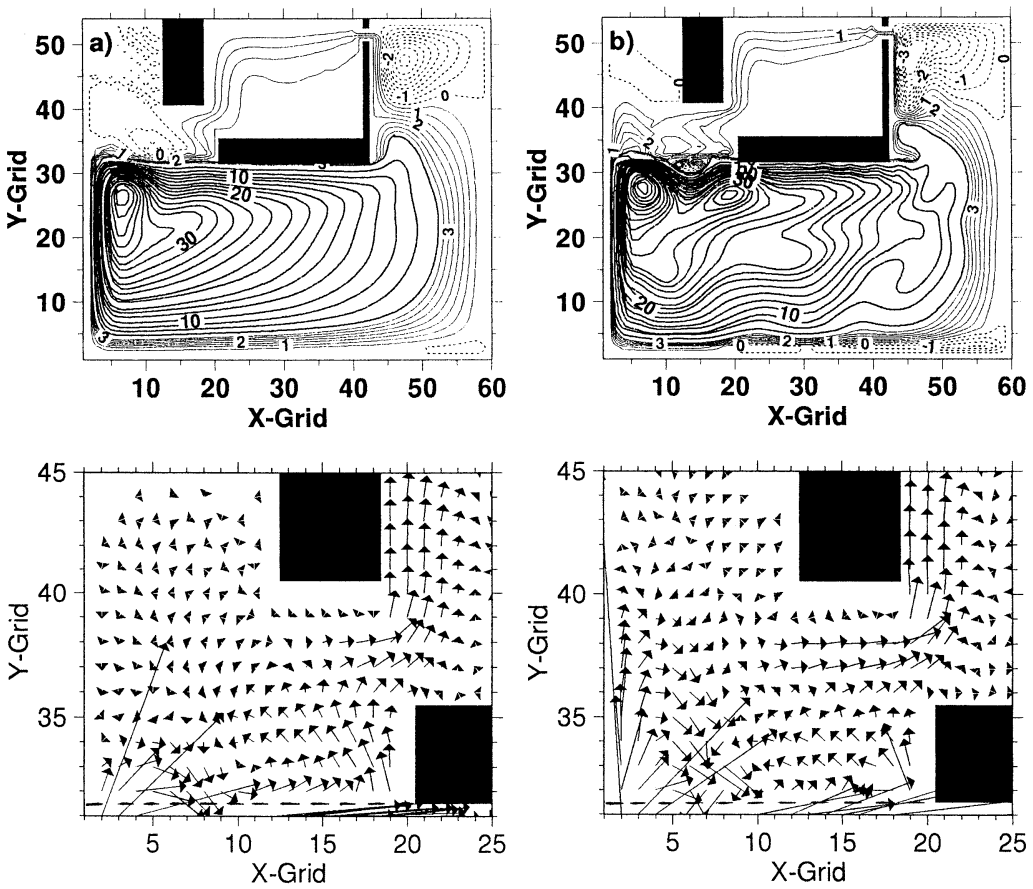

Fig. 6. Contours of streamfunction in Sv ($\times 10^6 m^3/s$) unit for a) EXP 6 (eddy viscosity coeff. : 5×10^7 cm^2/sec) and b) EXP 7 (eddy viscosity coeff. : 1×10^7 cm_2/sec). Lower panels are enlarged currents in the continental shelf region. The dashed line denotes the shelf break.

1994). This study, however, suggests that the existence of the deep trough west of Kyushu Island does not result in the branching from the Kuroshio, but acts to shift the separation position to the west of the trough.

To investigate any changes in the separation position of the WBC as the WBC becomes more inertial, the horizontal eddy viscosity is reduced in EXP 6 and EXP 7 to an half and one tenth the standard value, respectively, with other conditions the same as in EXP 1. As the inertial effect increases the recirculating subgyre in the northwestern corner of the deep ocean is intensified and moves further to the north. For a highly inertial case of EXP 7, two sub-gyres emerge south of the shelf break in the deep ocean as in Fig. 6b. The WBC becomes stronger and narrower and its transport is larger than the results of the standard experiment. The penetration of the WBC in EXP 6 takes place in area B nearly the same position as that in the standard experiment but in two areas in EXP 7; the area A and B. As the WBC becomes more inertial, the meridional scale of penetration of the WBC onto the shelf increases and the WBC reaches further to the north along the western wall of the shelf. This branch sharply turns anticyclonically over the shelf and part of it enters the MS while part of it returns to the WBC. The branching of the WBC also occurs in area B, hence the inflowing water into the MS comes from two areas in EXP 7. Observations show that part of the Kuroshio overruns the shelf break northeast of

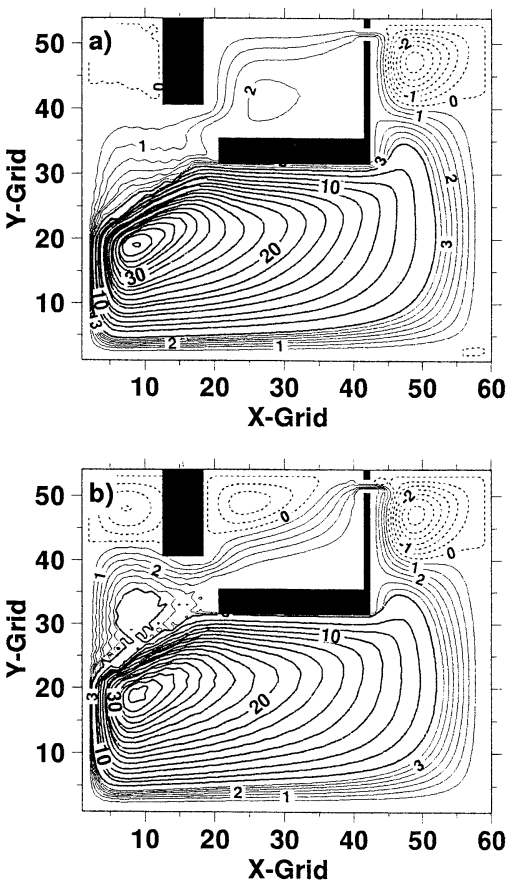

Fig. 7. Contours of streamfunction in Sv ($\times 10^6 m^3$/s) unit for a) EXP 8 and b) the barotropic version with all parameters the same as in EXP 8. The contour intervals are 0.5 Sv between -4 Sv to 4 Sv and 2 Sv elsewhere. The dashed lines denote the negative values of streamfunction.

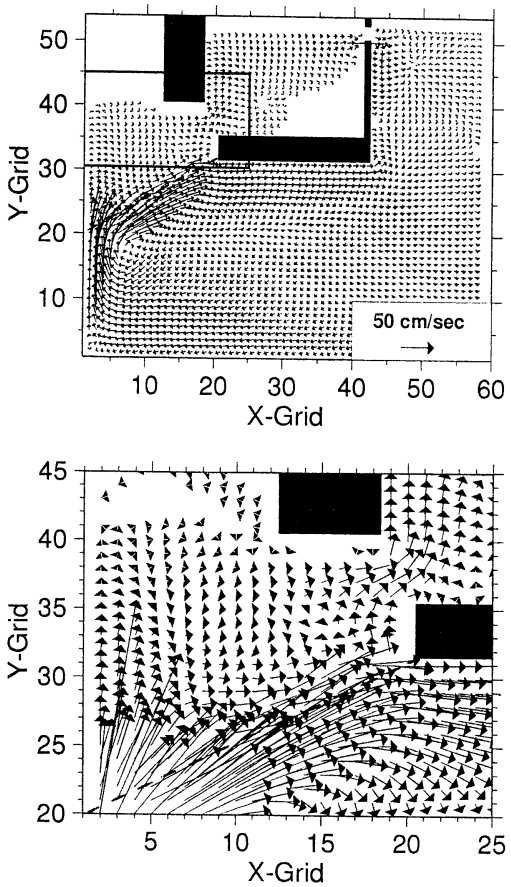

Fig. 8. Plots of currents at 75 m in EXP 8. Lower panels are enlarged currents in the continental shelf region. The dashed line denotes the shelf break.

Taiwan and turns anticyclonically as it impinges upon the continental slope (e.g. GUO and LIN, 1987), which is similar to the result of EXP 7. The result of EXP 7 is similar to that of the barotropic version of EXP 1 in that the penetration of the WBC onto the shelf takes place in area A. However, two different features also emerge; the penetration of a part of the WBC also takes place in area B and there exists a cyclonic circulation between area A and B.

Within the parameter range in Table 2 (EXP 2, 3, 9, 11) the separation position of the WBC is not affected by the maximum wind stress in the deep ocean and the depth ratios between the deep ocean and the shelf (not shown), it takes place in area B the same as the result of EXP 1. However, it should be noted that the separation position would be changed as the wind stress in the deep ocean further increases since the nonlinearity of the WBC depends on the wind stress applied as well as the eddy viscosity.

When the orientation of the shelf break is horizontally inclined (EXP 8), the stream line penetrates onto the continental shelf along the western boundary (area A). Part of it returns to the WBC and others flows into the MS. We can find the stream line which joins with the WBC and separates at the southwestern tip of the island again in Fig. 7 and the northward flow along the western boundary of the island (area B) in Fig. 8. The separation from the

WBC takes place both in area A and area B as shown in Fig. 8, which is markedly different from the result of the standard experiment with a zonally oriented shelf break. The flow pattern on the shelf is more or less similar to the result of a highly inertial case of EXP 5 and the inflow into the MS comes from both area A snd area B except that the cyclonic recirculation between area A and B cannot be seen in Exp 8 (Fig. 7a).

The stratification acts to decrease the influx to the MS the same as in the zonally-oriented shelf break case. The flow on the shelf has a broad feature for the stratified case, while the streamlines are more closely spaced for the homogeneous case.

4. Volume transport of the inflow into the MS

The transport of the WBC is increased by the vertical stratification of the WBC, but the transport into the MS is inversly decreased as mentioned previously. The volume transports of the WBC in EXP 1 and its barotropic version about 40 Sv and 36 Sv, respectively. The volume transports into the MS in EXP 1 and its barotropic version are about 1.86 Sv and 2.8 Sv, about 4.7% and 7.8% of the volume transport of the WBC respectively.

Figure 9 shows the dependence of the influx into the MS on some factors. Numerical experiments indicate that the influx is little sensitive to the orientation of the shelf break and the existence of the deep trough west of the MS. Instead, it is sensitive to the maximum wind stress in the deep ocean (or the volume transport of the WBC) and the depth ratio between the deep ocean and the shelf. The influx into the MS increases linearly as the transport of the WBC increases and the depth ratio decreases as shown in Fig. 9a and 9c, whch has been also shown in previous barotropic model results (MINATO and KIMURA, 1980; SEUNG and NAM, 1992; CHANG, 1993). As the nonlinear effect of the WBC increases, the WBC becomes narrower and stronger as can be seen in Fig. 6. The influx into the MS, however, changes only a little as the nonlinearity of the WBC increases. As the eddy viscosity decreases the influx slightly increases as shown in Fig. 9b.

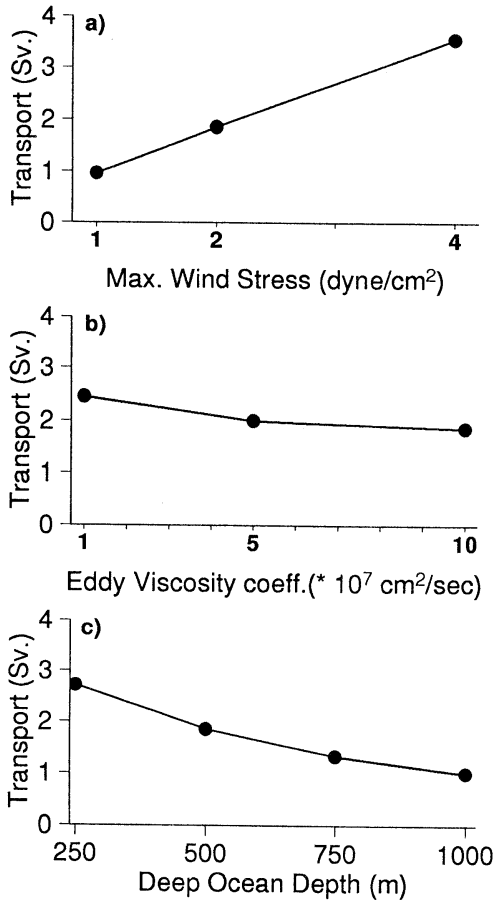

Fig. 9. Dependences of transport into the MS on a) the maximum wind stress applied over the deep ocean, b) the eddy viscosity coefficient, and c) the depth of the deep ocean.

5. Summary and Discussion

This study attempts to investigate the circulation of a continental shelf and a marginal sea driven by the WBC and highlights the variability of their circulation depending on the stratification, nonlinearity of the western boundary current and the orientation of the shelf break. The major circultion feature is such that part of the western boundary penetrates onto the shelf and enters the marginal sea while most of it follows the shelf break. The resulting shelf circulation and the influx to the marginal sea are dependent on various factors

For a zonally oriented shelf break, the separation from the WBC takes place in the eastern part of the shelf (area B) and the circulation on

the continental shelf is characterized by a weak cyclonic circulation, which differs from the result of the barotropic version of the standard experiment where the branching occurs in the western part of the shelf and the shelf circulation is anticyclonic. The separation, however, takes place along the western wall of the continental shelf even for the stratified case when the western boundary current becomes highly inertial, similar to the barotropic case. The branching position is also changed by the orientation of the shelf break. When the shelf break is oriented in the northeast direction, the separation occurs at two positions; one is area A and the other is area B. The definite dynamics for the alteration of the separation position of the western boundary current is left unexplained.

The amount of the inflow into the marginal sea is about 2 Sv, approximately 5% of the total volume transport of the western boundary current. It has been shown that the total volume transport of the western boundary current increases when the stratiFIcation is taken into account. On the other hand, the stratification acts to decrease the amount of the inflow to the marginal sea. According to the result of the standard experiment, an anticyclonic circulation and a weak cyclonic circulation are estabilished in the deep ocean and the continental shelf respectively with the thermal front in between them. The thermal front and stratification seem to play a role in blocking the penetration of the deep ocean water onto the shelf and the marginal sea in area A.

Numerical experiments show that the amount of the inflow to the marginal sea increases as the transport of the western boundary current increases and the depth ratio between the deep ocean and the shelf decreases as other studies suggested (SEUNG and NAM, 1992; MINATO and KIMURA, 1980; CHANG, 1993). The influx is only a little affected by the eddy viscosity. The orientation of the shelf break and specific topographic features of the shelf beak like the deep trough west of Kyushu do not affect the influx to the marginal sea.

It can be suggested from the present study that the branching of the Tsushima Current in the East China Sea can take place in the two regions; the western region of Kyushu and the northeastern region of Taiwan since the shelf break in the East China Sea is oriented in the northeast direction and the Kuroshio is likely to be inertial.

Acknowledgments

This study in mostly supported by grants from the Ministry of Science and Technology and the Ministry of Environment of Korea (PN00271-2) and partly supported by the Ministry of Science and Technology of Korea (PN00281-2, PN00278-7, PN00520).

Reference

BEARDSLEY, R. C., R. LIMEBURNER, H. YU and G. A. CANNON (1985): Discharge of the Changjiang into the East China Sea. Continental Shelf Res., **4**, Nos 1/2, 57-76.

CHANG, K.-I. (1993): The shelfward penetration of western boundary currents. Ph.D. thesis, dept. of oceanography, Southampton University.

CHAO, S.-Y. (1991): Circulation of the East China Sea, A Numerical Study. J. Oceanogr. Soc. Japan, **46**, 273-295.

COX, M. D. (1984): A primitive equation three-dimensional model of the ocean, Tech. Rep. 1,250pp., Geophys. Fluid Dyn. Lab., NOAA Princeton Univ., Priceton, N.J.

HSUEH, Y. (1986): The intrusion of the Kuroshio across the continental shelf northeast of Taiwan. J. Geophys. Res., **97** (C 9), 14323-14330.

GUAN, B. (1986): On the Circulation in the East China Sea. Studia Marina Sinica, **27**, 1-21.

GUO, B. and K. LIN (1987): Characteristics of circulation in the continental shelf area of the East China Sea in winter. Acta Oceanologica Sinica, V. **6**, Supp. I, 51-60.

GUO, B., S. XIU, H. ISHII and Y. NAKAMURA (1990): Kuroshio warm filament and the source of the warm water of the Tsushima Current. Proc. of Japan China Joint Symp. of the Cooperative Study on the Kuroshio, 112-127.

HOLLAND W. R. (1973): Baroclinic and topographic influences on the transport in the western boundary currents. Geophys. Fluid Dyn., **4**, 187-210.

ICHIKAWA, H. and R. C. BEARDSLEY (1993): Temporal and spacial variability of volume transport of the Kuroshio in the East China Sea. Deep Sea Research, **40** (3), 583-605.

LIE H. J. and C. H. CHO (1994): On the origin of the Tsushima Cureent. J. Geophy. Res., **99**, 25081-25091.

LIE, H. J. *et al.* (1993): Study on oceanographic variability in the formation area of the Tsushima warm Current. KORDI, BSPN 00179-603-1, 193 pp.

LIM D. B. (1971): On the origin of the Tsushima Current Water. J. Oceanogr. Soc. Korea, **6**, 85-91.

MIITA T. and Y. OGAWA (1984): Tsushima Currents measured with current meters and drifters. In Ocean Hydrodynamics of the Japan and East China Seas. T. ICHIYE (ed.), Elsevier, 235-352.

MINATO, S. and R. KIMURA (1980): Volume transport of the Western boundary current penetrating into a marginal sea. J. Oceanogr. Soc. Japan, **36**, 185-195.

MORIYASU, S. (1972): The Tsushima Current. In Kuroshio: Its physical Aspects. by H. STOMMEL and K. YOSHIDA (eds), Univ. of Washington Press, 353-369.

NAM S. Y. and Y. H. SEUNG (1992): A numerical model on the inflow into the Japan Sea: the formation and transport of the Tsushima Warm Current. Bull. Korean Fish. Soc., **25**, 58-64.

NOF, D. (1993): The penetration of Kuroshio into the Sea of Japan. J. Phys. Oceanogr., **23**, 797-807.

OEY, L-Y. and P. CHEN (1991): Frontal waves upstream of a diabathic blocking: A model study. J. Phys. Oceanogr., **21** (11), 1643-1663.

SEUNG, Y. H., and S. Y. NAM (1992): A numerical study on the barotropic transport of the Tsushima Current, La mer, **30**, 139-147.

TAKANO, K. (1974): A general circulation model for the world ocean. UCLA Dept. of Meteorology Tech. Rep. No.8.

TAKANO, K and A. MISUMI (1990): Numerical simulation of the North Pacific circulation as a fundmental study on the Kuroshio power harnessing. Proc. Japan-China Joint Res., STA (Japan) and SOA (China), 146-156.

YI, S. U. (1996): Seasonal and secular variations of the water volume transport across the Korea Strait. J. Oceanol. Soc., Korea, **1**, 7-13.

Received January 9, 1996
Accepted March 11, 1996